

## ARTICLE OPEN



# Buffer induced ionically crosslinked polyelectrolyte treatment for self-extinguishing polyester

Dallin L. Smith<sup>1</sup>, Natalie A. Vest<sup>1</sup>, Miguel O. Convento<sup>2</sup>, Maya D. Montemayor<sup>1</sup> and Jaime C. Grunlan<sup>1,2,3</sup>✉

Over 60 million tons of polyethylene terephthalate (PET) fibers are produced annually for clothing, upholstery, linens, and carpeting. Despite its widespread use, the versatility of PET is constrained by its flammability, which poses a particular fire hazard to homes with synthetic furnishings. To mitigate this fire risk, a polyelectrolyte complex (PEC) solution composed of polyallylamine hydrochloride and poly(sodium phosphate) is deposited onto the surface of 100% polyester fabric to render it self-extinguishing and eliminate melt dripping. A buffered solution of acetic acid, citric acid, or formic acid is used to initiate ionic complexation, rendering the PEC water resistant. Buffer identity affects deposition, but does not significantly influence the intumescent mechanism. This rapidly deposited aqueous coating primarily operates by facilitating production of an insulating char layer that limits the heat release and degradation of polyester into volatile byproducts.

*npj Materials Degradation* (2024)8:14; <https://doi.org/10.1038/s41529-024-00432-2>

## INTRODUCTION

Polyester, most commonly polyethylene terephthalate (PET), accounts for a majority of global fiber production, with over 60 million tons of PET fibers produced in 2021<sup>1</sup>. Polyester's chemical, mechanical, heat, and wrinkle resistance (and compatibility with cotton in blends) make it very popular in clothing and furnishings<sup>2–4</sup>. Unfortunately, polyester forms molten droplets and exhibits high heat release when it burns, both of which exacerbate fire risk and propagation. The growing prevalence of synthetic materials in homes poses a growing challenge for firefighters<sup>5–7</sup>.

Several approaches can be taken to address the flammability of polyester, including copolymerization with flame retardant monomers<sup>8,9</sup>, extruding with flame retardant additives<sup>10–13</sup>, or applying flame retardant coatings<sup>2,3,14–16</sup>. Although the first two methods produce an inherently flame retardant (FR) material, they are not without challenges. Copolymerization can alter the polymerization kinetics and thermal, mechanical, or electrical properties of the final polymer<sup>5</sup>. Additionally, small molecule additives and fillers can leach out of the polymer over time, which could pose risk to human or environmental health (especially if halogenated) and reestablish initial fire risk. Either approach can impair recyclability of the polyester as well<sup>17</sup>, of which only 15% of global fiber production comes from recycled material<sup>1</sup>. Due to these limitations, surface coatings are often used as a facile solution for flammable textiles.

Flame retardant surface coatings typically function via intumescence and/or passive barrier<sup>17</sup>. These coatings operate in the gas phase by diluting flammable volatiles and/or the condensed phase by forming an insulating char layer on the substrate. Layer-by-layer assembly facilitates a virtually limitless array of FR chemistries<sup>18–22</sup>, but the number of processing steps required is a significant drawback. In contrast, 'OnePot' polyelectrolyte complexes (PECs) can be deposited in one or two steps by inducing entropy-driven complexation between the polyelectrolytes. This can be accomplished by manipulating the ionic strength or pH of the aqueous environment, such as with an acidic buffer. Intumescent PECs have been applied in this way to

cellulosic and synthetic polymers<sup>3,23–28</sup>. Compared to cellulosic fabrics, polyester is hardly able to form char, so an intumescent treatment must provide a sufficient source of carbon to achieve a protective thermal barrier during burning.

Poly(allylamine hydrochloride) (PAH) and poly(sodium phosphate) (PSP) have been paired as intumescent polyelectrolytes for cotton and polyester/cotton blended fabrics<sup>24,29</sup>. At pH values above the  $pK_a$  of polyallylamine (8.5–9), the two polymers form a stable suspension<sup>24,30</sup>. Ionic complexation can be induced in-situ upon submersion in an acidic buffer, which charges the primary amines on PAH (Fig. 1). In a similar system on cotton, lower pH buffers resulted in higher phosphorus content, which produced better FR results<sup>23</sup>. It has been presumed that residual buffer is removed by a subsequent deionized water rinse and therefore does not contribute to the FR mechanism of the coating. Citric acid is typically used<sup>23,24,26,27,31,32</sup>, but other affordable weak acids are available. To our knowledge, the relationship between buffer chemistry (i.e., structure and acidity) and PEC deposition or FR efficacy has not been thoroughly examined.

In this study, three weak acids with varying acidity and buffer capacity at pH 3 (acetic, citric, and formic) are paired with a PAH/PSP coating to render 100% PET self-extinguishing. Polyelectrolyte-based intumescent systems are often applied and well-studied on cellulosic substrates, but less often on poor char-forming synthetic fabrics such as polyester. On PET, the FR coating primarily operates in the condensed phase, limiting burning and degradation by constructing a barrier of char. Various analyses indicate the properties of the fabric are dominated by the PEC itself, rather than the buffer used for ionic crosslinking. Acetic and formic acids render PET self-extinguishing with lower weight gain than a citric acid buffer due to their lower buffer capacity. Intumescence is exhibited by accelerated decomposition and improved char formation accompanied by a decrease in total heat release. This system demonstrates scalable fire protection for a synthetic textile without detriment to the fabric's hand or the environment.

<sup>1</sup>Department of Chemistry, Texas A&M University, College Station, TX 77843, USA. <sup>2</sup>Department of Mechanical Engineering, Texas A&M University, College Station, TX 77843, USA. <sup>3</sup>Department of Materials Science and Engineering, Texas A&M University, College Station, TX 77843, USA. ✉email: [jgrunlan@tamu.edu](mailto:jgrunlan@tamu.edu)

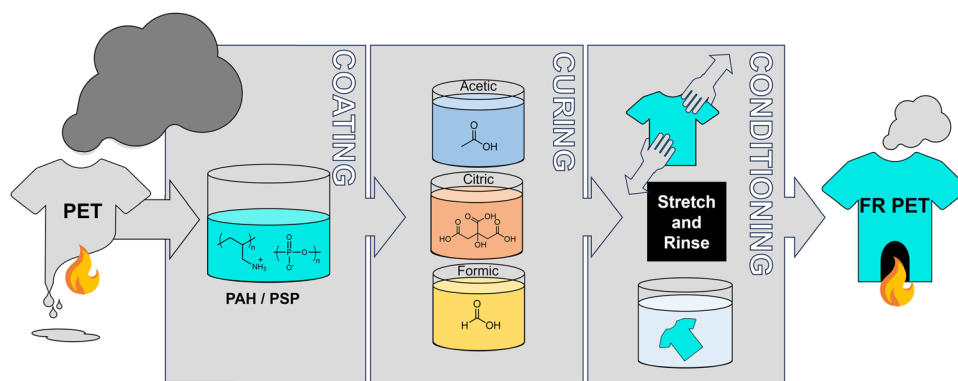


**Fig. 1 Application of PEC.** Schematic of the polyester coating process, including PEC deposition, ionic curing in a weak acid, and subsequent stretching and rinsing.

	Acetic	Citric	Formic
$pK_a$ Value(s)	4.76	3.13, 4.76, 6.40	3.75
Weight Gain (%)	$27.7 \pm 2.3$	$40.4 \pm 1.6$	$24.3 \pm 1.3$
C:P	10.91	16.18	14.54
P:N	0.92	0.73	0.91
O:P	3.78	4.54	4.77

## RESULTS AND DISCUSSION

### Coating deposition

The primary role of the buffer is to act as a source of protons for polyallylamine, which forms an ionic complex with polyphosphate when charged. It is expected that an acid with higher buffer capacity would yield a larger amount of PEC deposited onto the polyester. The amount of PEC deposited onto the polyester is similar for acetic acid and formic acid but is much higher for citric acid (Table 1). Acetic acid and formic acid are very similar in structure, but acetic acid has decreased acidity due to the destabilizing effect of the  $-\text{CH}_3$  group. This difference in  $pK_a$  results in a lower percent ionization at pH 3 for acetic acid, which could explain the slightly higher weight gain. Citric acid has an additional acidic proton, which increases its buffer capacity and ability to charge polyallylamine during submersion in the buffer. Compositional differences between coatings were studied using XPS. As observed in other polyamine/polyphosphate PECs, the P:N ratio is  $< 1$  for each system<sup>23,24</sup>. This indicates a stoichiometric excess of polyallylamine. Excess positive charge could be neutralized by pairing with the conjugate base of each buffer acid (i.e., acetate, citrate, formate), thus incorporating the buffer within the coating. The citric acid-cured coating has a lower P:N and higher O:P ratio, which could arise from the potential displacement of PSP by citrate.

For any surface treatment on a textile, the influence on the hand of the fabric needs to be considered. To restore the original hand of the PET, each sample was manually stretched after the buffer and rinse step. A final rinse in DI water was performed to remove any dislodged material. Although the mass loss from this process is negligible ( $\sim 30$  mg,  $< 1\%$ ), the hand is dramatically improved (Supplementary Fig. 1). To quantify mechanical strength, tensile testing was performed on each type of sample in triplicate (Supplementary Fig. 2). For coatings complexed by acetic acid and formic acid, the tensile strength and elongation-at-break of the polyester are no different than uncoated polyester. Citric acid reduces elongation-at-break, likely due to the higher amount of PEC deposited. In SEM images, a small amount of fiber bridging accompanies conformal deposition for samples cured by

acetic acid and formic acid. On the other hand, citric acid leaves microscopic particles of PEC amidst polyester fibers, showing that excess deposition will inevitably be shed from the fibers during manipulation (Fig. 2).

### Fire Performance

Uncoated polyester is flammable, but it melts away from a flame and forms no charred residue<sup>2,3</sup>. In contrast, each coated polyester sample self-extinguishes in vertical flame testing (VFT) and forms visibly charred residue (Supplementary Fig. 3). The results from VFT are summarized in Table 2. Although citric acid deposits the highest amount of PEC, there appears to be no benefit over the other two systems, which exhibit no afterburn and slightly shorter charred lengths. As expected, given their chemical structures and comparable weight gains on the fabric, acetic acid and formic acid produce similar fire performance.

SEM imaging was performed on the burned residue to investigate the mechanism of action. In uncoated polyester, the transition from fibers to a homogenous melt is observed (Fig. 3). Fiber structure remains faintly identifiable in the residues of coated PET due to the protective coating. The PEC significantly improves the ability of the polyester to char, which on its own can only form a limited amount via crosslinking of polymerized degradation products<sup>15,33</sup>. Phosphorus compounds promote char formation by producing thermally stable P–O–C bonds and increase the aromaticity of the residue<sup>12,26,34,35</sup>. In addition to the substrate itself, nitrogen compounds act as blowing agents to swell the char, which is evident by the bubbles observed in SEM images. In each case, evidence of intumescent condensed phase and gas phase action is apparent in all coated samples.

### Thermal degradation

Nonoxidative thermal degradation of the samples was studied using thermogravimetric analysis under argon (Fig. 4). Polyester undergoes a single degradation step from 400 to 450 °C and leaves only  $\sim 10\%$  residue at 600 °C, which is the product of crosslinked vinyl esters or self-condensation of aldol products (Table 3)<sup>34</sup>. The temperature at which coated samples begin to degrade ( $T_{5\%}$ ) begins 50–150 °C earlier, which is typical (and essential) for an intumescent coating<sup>17</sup>. Similarly, the temperature at which maximum mass loss rate occurs ( $T_{\text{max}}$ ) is 40 °C lower regardless of buffer acid used, which suggests the shift arises due to the PEC itself, not the buffer. In addition, the residue at 600 °C is more than doubled by the coatings, which suggests a condensed phase mechanism that allows char to form. The accentuated shoulder for citric acid ( $\sim 430$  °C) is attributed to its higher PEC content.

Microscale combustion calorimetry determines the heat release of a material based on the amount of oxygen consumed by

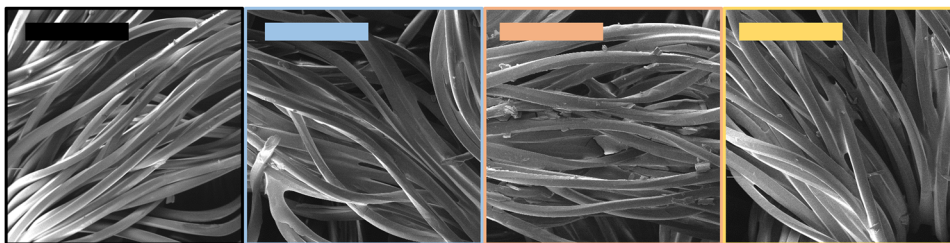


**Fig. 2 PEC deposition.** SEM images of polyester fibers treated with no coating (black), acetic acid (blue), citric acid (orange), or formic acid (yellow). Scale bars are 200  $\mu\text{m}$ .

**Table 2.** Vertical flame test results for uncoated and coated PET.

Sample	Residue (%)	Afterburn (sec)	Damaged Length (cm)
Uncoated	90.5 $\pm$ 4.6	18.7 $\pm$ 5.6	13.2 $\pm$ 1.9
Acetic	96.8 $\pm$ 0.5	0.0 $\pm$ 0.0	11.9 $\pm$ 0.2
Citric	97.0 $\pm$ 1.1	3.7 $\pm$ 3.3	14.0 $\pm$ 1.8
Formic	95.8 $\pm$ 0.5	0.0 $\pm$ 0.0	13.7 $\pm$ 1.2

volatile pyrolysis products, so it provides insight into gas phase action of an intumescent system. Since pyrolysis and combustion are decoupled in MCC, results are not indicative of real fire conditions<sup>36</sup>, but it complements VFT and other degradation analyses by providing parameters such as peak heat release rate (pkHRR), total heat release (THR), and peak heat release rate temperature ( $T_{\text{pkHRR}}$ ). Like TGA, MCC shows that each buffered coating accelerates the release of initial pyrolysis products by as much as 50  $^{\circ}\text{C}$  (Fig. 5). Again, there is no significant difference between acetic acid and formic acid buffered systems, but citric acid exhibits lower pkHRR, attributed partly to its greater PEC deposition. THR is lowered by up to 30%, but pkHRR is not reduced for the buffered samples (Table 4). Typically, the accelerated degradation observed in intumescent coatings is accompanied by a reduction in heat release, due to the insulation of the underlying substrate by a carbonaceous barrier, whether or not the substrate is cellulosic<sup>2,3,15,23–27,35</sup>. All three buffered systems improve the char yield by  $\sim$ 200%, which coincides with the condensed phase action observed in SEM and TGA. The reduced THR can be explained by the formation of char acting as a physical barrier to heat and mass transfer, which prevents total degradation and protects the residual polyester from fire<sup>2,15,24</sup>. Though fewer volatiles are generated as a result, pkHRR remains high due to volatiles produced before and during char development. Even with some increase in pkHRR, fire growth capacity (FGC), which is a measure of a material's potential to ignite and increase fire intensity, is reduced for all samples<sup>37</sup>.

Principal thermal degradation products of polyester are acetaldehyde, carbon monoxide, carbon dioxide, benzene, toluene, styrene, and benzoic acid<sup>33,38,39</sup>. Mass spectrometry was coupled with TGA to compare volatile production for each polyester sample. Production of acetaldehyde/carbon dioxide (44 amu), benzene (78 amu), styrene (104 amu), and benzoic acid (122 amu) is clearly evident from 400 to 500  $^{\circ}\text{C}$  for uncoated polyester, whereas normalized emission of these byproducts is significantly reduced in each buffered sample (Fig. 6). Additionally, increased water emission corresponds to the formation of char via aldol condensation reactions catalyzed by phosphorus<sup>40</sup>. No significant difference between coated systems is apparent in TGA-MS, so if buffer remains in the system, it does not appear to affect degradation. For each thermal analysis technique performed (i.e., VFT, TGA, MCC), the three systems result in similar percent residues, indicating a comparable degree of condensed phase action or char produced. As mentioned earlier, reduced

emission of combustible volatiles by the coated samples corresponds with a lower THR in MCC. Despite fewer PET degradation products being released, pkHRR for the coated samples is not lowered. As a result, it can be concluded that the FR system simultaneously contributes to heat release via other products (e.g., HCN), but ultimately reduces overall heat release.

To address the fire hazard polyester poses, a rapidly-applied, water-based polymeric surface coating was applied. Without altering the mechanical properties of the fabric, this coating renders PET self-extinguishing and completely prevents melt dripping by establishing a robust char layer that stops afterburn. The polyelectrolyte complex (PAH/PSP) is deposited conformally in an amount influenced by the weak acid used. The fire performance is largely dictated by the PEC itself, with small variations between systems complexed by different acids. The buffer acid does not affect the degradation chemistry, but it does influence deposition, which leads to minor differences in fire performance. As with many intumescent systems, substrate degradation is accelerated by this coating to provide an insulating char that prevents further degradation in oxidative or non-oxidative environments. As a result, total heat release and fire growth capacity of polyester are reduced by up to 30% and 37%, respectively. Similarly, the emission of flammable byproducts is cut by more than half. This highly effective and environmentally benign treatment holds tremendous potential for protecting a variety of clothing and upholstery from fire.

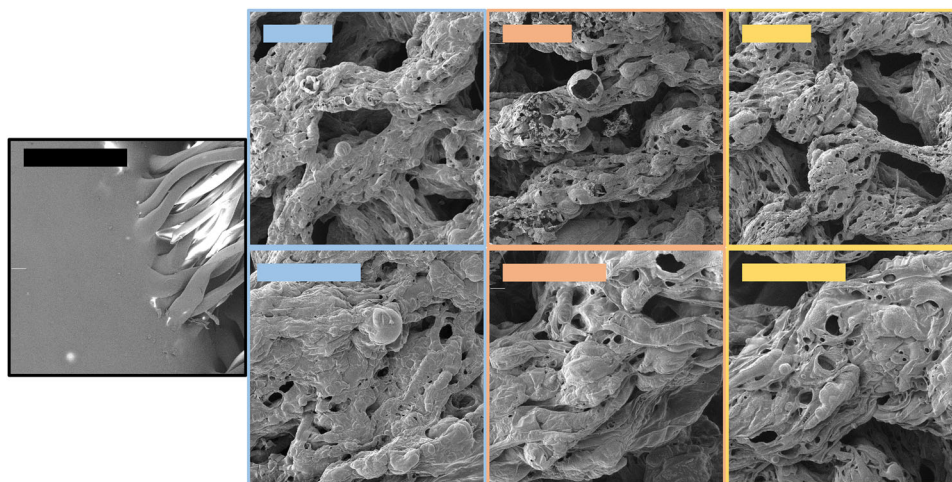
## METHODS

### Materials

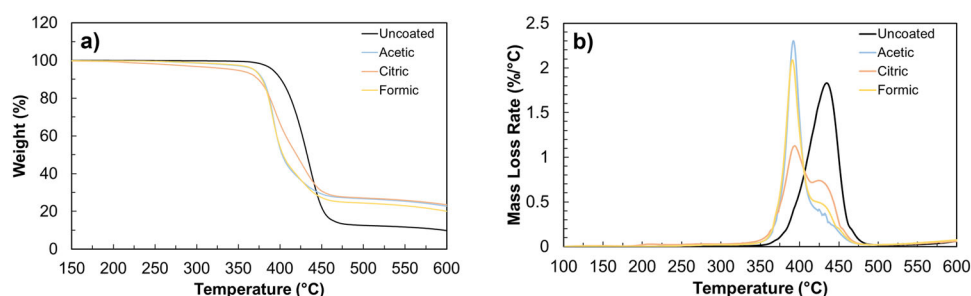
Polyester fabric, with a weight of 200  $\text{g} \cdot \text{m}^{-2}$ , was purchased from TestFabrics, Inc (West Pittston, PA). Poly(allylamine hydrochloride) (PAH,  $M_w = 15,000 \text{ g} \cdot \text{mol}^{-1}$ ) was purchased from Beckmann-Kenko (Bassum, Germany). Poly(sodium phosphate) (PSP) (crystalline, 96%), glacial acetic acid, citric acid monohydrate ( $\geq 98\%$ ), formic acid ( $\geq 98\%$ ), hydrochloric acid (HCl, 37% solution), and sodium hydroxide (NaOH,  $\geq 98\%$ ) were purchased from Millipore-Sigma (Burlington, MA). All solutions were made with 18 M $\Omega$  deionized (DI) water.

### Fabric coating

Fabrics were rinsed thoroughly with DI water and dried at 70  $^{\circ}\text{C}$  before coating. To make the PEC, a 23.5% (w/w) solution of PAH was prepared in DI water with an equimolar amount of NaOH pellets (to neutralize the HCl), and an equal weight of a 25.5% (w/w) PSP solution was added during magnetic stirring. To make the buffer, the acid was added to water and the pH was adjusted to 3.0 using 5 M NaOH or 5 M HCl, before diluting with the appropriate amount of DI water to yield a final concentration of 0.2 M. The polyester was submerged in the PEC for 1 min, squeezed to remove excess liquid, and dried at 70  $^{\circ}\text{C}$ . PEC complexation was then induced by submerging the fabric in a single buffer solution for 1 min, and the fabric was thoroughly rinsed in DI water and dried at 70  $^{\circ}\text{C}$ . Next, the polyester was manually stretched in both



**Fig. 3 Post-burn residue.** SEM images of polyester fibers after VFT: no coating (black), acetic acid (blue), citric acid (orange), and formic acid (yellow) buffered PEC. Scale bars in top row are 400  $\mu\text{m}$ , while scale bars for no coating and bottom row are 200  $\mu\text{m}$ .



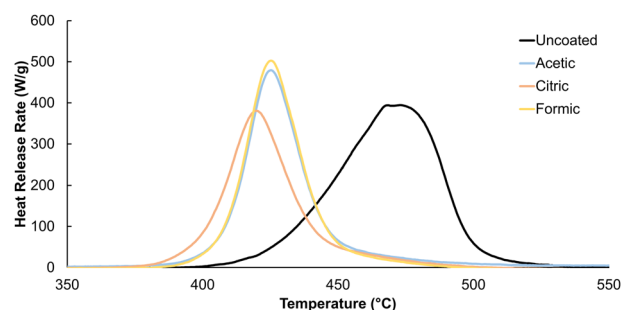
**Fig. 4 TGA curves.** Weight loss (a) and derivative weight loss (b) as a function of temperature for polyester samples.

Table 3. Thermal degradation parameters for each polyester under argon.			
Sample	$T_{5\%}$ ( $^{\circ}\text{C}$ )	$T_{\text{max}}$ ( $^{\circ}\text{C}$ )	Residue at 600 $^{\circ}\text{C}$ (%)
Uncoated	389.0	434.5	9.7
Acetic	346.1	392.2	22.2
Citric	244.6	393.8	22.7
Formic	354.2	390.8	19.6

directions, rinsed, and dried once more. This deposition process is summarized in Fig. 1.

### Characterization

Mechanical testing was performed on 1-inch strips of fabric using an Instron 6800 Universal Testing Machine (Norwood, MA), with an initial clamp displacement of 5.0 cm and strain rate of 10.0  $\text{mm}\cdot\text{min}^{-1}$ . Scanning electron microscope (SEM) images were obtained on a VEGA instrument (Tescan Orsay Holding, Czech Republic) with 5 kV beam voltage. Samples were prepared for imaging by depositing a 5-nm thick Au layer by sputter-coating (Cressington Scientific Instruments, United Kingdom). X-ray photoelectron spectroscopy (XPS) spectra were acquired with an Omicron X-ray photoelectron spectrometer (Denver, CO), with a DAR 400 Mg X-ray source and a 0.8 eV energy resolution Argus detector. 3-4 spectra were averaged and analyzed using CasaXPS software. Fire performance was evaluated using the ASTM D6413 standard 12 s vertical flame test (VFT) in a VC-2

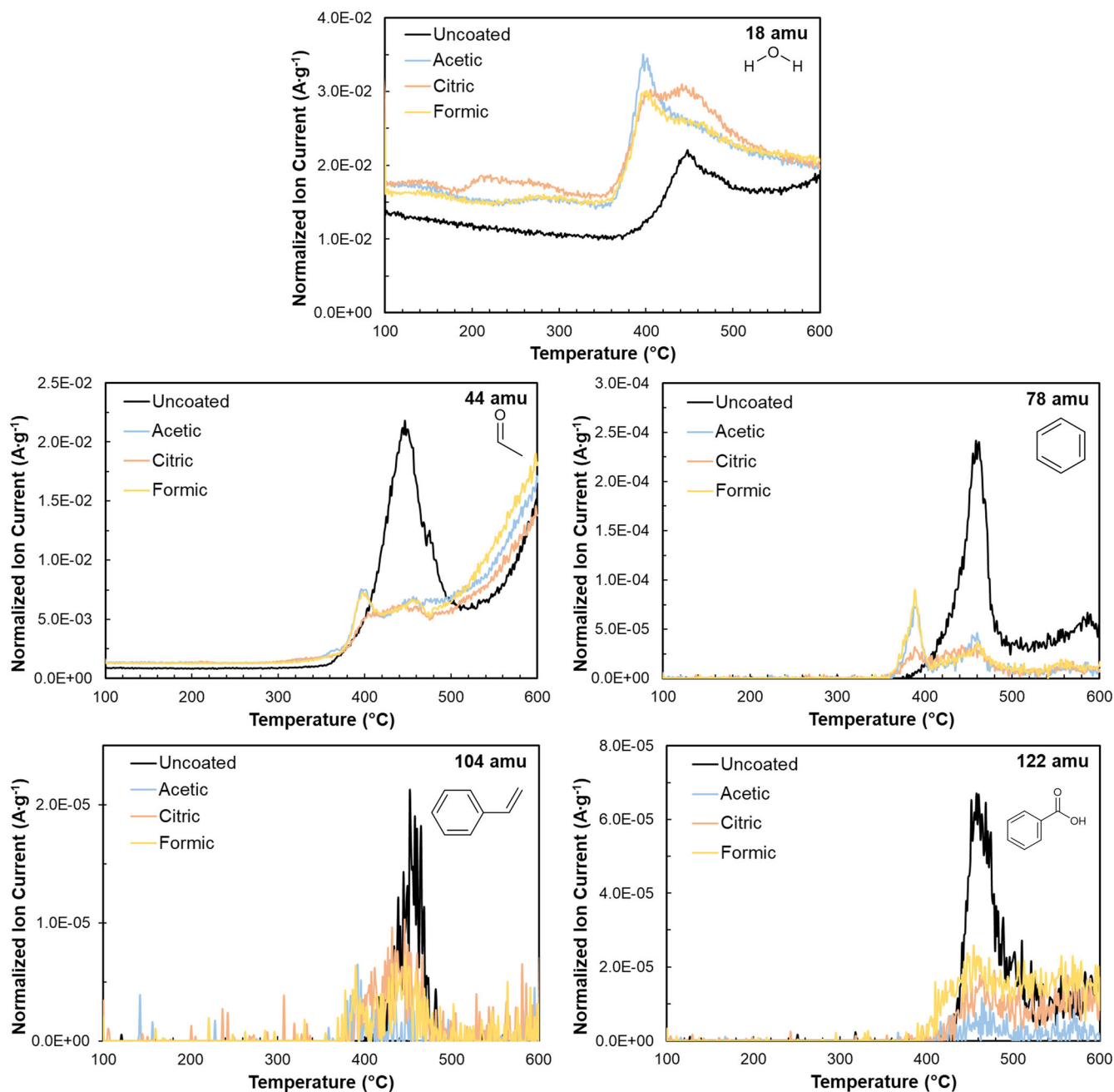


**Fig. 5 MCC curves.** Representative microscale combustion calorimetry curves for each polyester sample.

model flame testing cabinet (Govmark, Farmingdale, NY). Thermal degradation and gas evolution were studied by thermogravimetric analysis-mass spectrometry (TGA-MS) on a TGA 5500 with a Discovery mass spectrometer (TA Instruments, New Castle, DE). Samples ( $\sim 5$  mg) were heated at a rate of 10  $^{\circ}\text{C}\cdot\text{min}^{-1}$  under argon with 25  $\text{mL}\cdot\text{min}^{-1}$  sample flow and 10  $\text{mL}\cdot\text{min}^{-1}$  purge flow, after being held at 100  $^{\circ}\text{C}$  for 20 minutes to remove residual water. Microscale combustion calorimetry (MCC) was performed according to Method A of ASTM D7309 (Deatak, McHenry, IL). Triplicate samples were heated at 1  $^{\circ}\text{C}\cdot\text{sec}^{-1}$  to 600  $^{\circ}\text{C}$  under a flow rate of 80  $\text{mL}\cdot\text{min}^{-1}$  nitrogen and the thermal degradation products were mixed with a 20  $\text{mL}\cdot\text{min}^{-1}$  stream of oxygen before entering a 900  $^{\circ}\text{C}$  combustion furnace.

**Table 4.** Microscale combustion calorimetry data.

Sample	Char Yield (%)	pkHRR ( $\text{W} \cdot \text{g}^{-1}$ )	$T_{\text{pkHRR}}$ ( $^{\circ}\text{C}$ )	THR ( $\text{kJ} \cdot \text{g}^{-1}$ )	FGC ( $\text{J} \cdot \text{g}^{-1} \cdot \text{K}^{-1}$ )
Uncoated	$8.0 \pm 3.6$	$392.8 \pm 1.2$	$470 \pm 4$	$18.3 \pm 0.9$	$352 \pm 8$
Acetic	$28.1 \pm 5.6$	$486.2 \pm 17.1$	$425 \pm 1$	$13.4 \pm 0.6$	$287 \pm 11$
Citric	$26.4 \pm 1.4$	$386.1 \pm 9.1$	$420 \pm 1$	$12.9 \pm 0.2$	$222 \pm 10$
Formic	$22.9 \pm 3.4$	$499.1 \pm 22.0$	$425 \pm 0$	$14.2 \pm 0.3$	$287 \pm 9$

**Fig. 6** Volatile emission. Mass spectrometry of major decomposition products of polyester during TGA under argon.

## DATA AVAILABILITY

Data supporting the findings of this study are available from the corresponding author upon request.

Received: 16 October 2023; Accepted: 14 January 2024;

Published online: 25 January 2024

## REFERENCES

1. Preferred Fiber & Materials Market Report. [http://textileexchange.org/app/uploads/2022/10/Textile-Exchange\\_PFMR\\_2022.pdf](http://textileexchange.org/app/uploads/2022/10/Textile-Exchange_PFMR_2022.pdf) (2022).
2. Jordanov, I. et al. Flame retardant polyester fabric from nitrogen-rich low molecular weight additives within intumescent nanocoating. *Polym. Degrad. Stab.* **170**, 108998 (2019).
3. Chen, F. et al. Fully bio-based flame retardant and antibacterial coating for polyethylene terephthalate fabric. *Prog. Org. Coat.* **182**, 107637 (2023).
4. Alongi, J., Carosio, F. & Kiekens, P. Recent advances in the design of water based-flame retardant coatings for polyester and polyester-cotton blends. *Polymers* **8**, 357 (2016).
5. Morgan, A. B. The future of flame retardant polymers – unmet needs and likely new approaches. *Polym. Rev.* **59**, 25–54 (2019).
6. Morgan, A. B. The well-meaning but misguided rollback of fire safety in the United States. *J. Fire Sci.* **40**, 249–253 (2022).
7. Newer homes and furniture burn faster, giving you less time to escape a fire. *TODAY.com*. <https://www.today.com/home/newer-homes-furniture-burn-faster-giving-you-less-time-escape-t65826> (2017).
8. Dong, X., Chen, L., Duan, R.-T. & Wang, Y.-Z. Phenylmaleimide-containing PET-based copolyester: cross-linking from  $2\pi + \pi$  cycloaddition toward flame retardant and anti-dripping. *Polym. Chem.* **7**, 2698–2708 (2016).
9. Zhao, H.-B. & Wang, Y.-Z. Design and Synthesis of PET-based copolyesters with flame-retardant and antidripping performance. *Macromol. Rapid Commun.* **38**, 1700451 (2017).
10. Salmeia, K. A. et al. Comprehensive study on flame retardant polyesters from phosphorus additives. *Polym. Degrad. Stab.* **155**, 22–34 (2018).
11. Gooneie, A. et al. Enhanced PET processing with organophosphorus additive: Flame retardant products with added-value for recycling. *Polym. Degrad. Stab.* **160**, 218–228 (2019).
12. Liu, B.-W., Zhao, H.-B. & Wang, Y.-Z. Advanced flame-retardant methods for polymeric materials. *Adv. Mater.* **34**, 2107905 (2022).
13. Zhang, L., Yi, D. & Hao, J. Poly (diallyldimethylammonium) and polyphosphate polyelectrolyte complexes as an all-in-one flame retardant for polypropylene. *Polym. Adv. Technol.* **31**, 260–272 (2020).
14. Fang, Y., Wu, J., Chen, Y. & Wu, L. Durable flame retardant and anti-dripping of PET fabric using bio-based covalent crosslinking intumescent system of chitosan and phytic acid. *Prog. Org. Coat.* **183**, 107785 (2023).
15. Wu, Y., Zhou, X., Xing, Z. & Ma, J. Metal compounds as catalysts in the intumescent flame retardant system for polyethylene terephthalate fabrics. *Text. Res. J.* **89**, 2983–2997 (2019).
16. Tao, Y. et al. A flame-retardant PET fabric coating: Flammability, anti-dripping properties, and flame-retardant mechanism. *Prog. Org. Coat.* **150**, 105971 (2021).
17. Lazar, S. T., Kolibaba, T. J. & Grunlan, J. C. Flame-retardant surface treatments. *Nat. Rev. Mater.* **5**, 259–275 (2020).
18. Holder, K. M., Smith, R. J. & Grunlan, J. C. A review of flame retardant nano-coatings prepared using layer-by-layer assembly of polyelectrolytes. *J. Mater. Sci.* **52**, 12923–12959 (2017).
19. Smith, D. L., Vest, N. A., Rodriguez-Melendez, D., Palen, B. & Grunlan, J. C. Bio-Sourced Intumescent Nanocoating. *Adv. Eng. Mater.* **25**, 2200911 (2023).
20. Wang, B. et al. Flame-retardant polyester/cotton blend with phosphorus/nitrogen/silicon-containing nano-coating by layer-by-layer assembly. *Appl. Surf. Sci.* **509**, 145323 (2020).
21. An, W., Ma, J., Xu, Q. & Fan, Q. Flame retardant, antistatic cotton fabrics crafted by layer-by-layer assembly. *Cellulose* **27**, 8457–8469 (2020).
22. Fang, Y., Sun, W., Liu, H. & Liu, X. Construction of eco-friendly flame retardant and dripping-resistant coating on polyester fabrics. *Surf. Eng.* **37**, 1067–1073 (2021).
23. Haile, M., Fincher, C., Fomete, S. & Grunlan, J. C. Water-soluble polyelectrolyte complexes that extinguish fire on cotton fabric when deposited as pH-cured nanocoating. *Polym. Degrad. Stab.* **114**, 60–64 (2015).
24. Haile, M. et al. A wash-durable polyelectrolyte complex that extinguishes flames on polyester–cotton fabric. *RSC Adv.* **6**, 33998–34004 (2016).
25. Leistner, M., Haile, M., Rohmer, S., Abu-Odeh, A. & Grunlan, J. C. Water-soluble polyelectrolyte complex nanocoating for flame retardant nylon-cotton fabric. *Polym. Degrad. Stab.* **122**, 1–7 (2015).
26. Vest, N. A. et al. Polyelectrolyte complex for flame retardant silk. *Polym. Degrad. Stab.* **216**, 110491 (2023).
27. Rodriguez-Melendez, D. et al. Two-Step Polyelectrolyte Complex Coating for Flame Retardant Flax. *Macromol. Mater. Eng.* **309**, 2300229 (2024).
28. Zhang, T. et al. A phosphorus-, nitrogen- and carbon-containing polyelectrolyte complex: preparation, characterization and its flame retardant performance on polypropylene. *RSC Adv.* **4**, 48285–48292 (2014).
29. Li, Y.-C. et al. Intumescent All-Polymer Multilayer Nanocoating Capable of Extinguishing Flame on Fabric. *Adv. Mater.* **23**, 3926–3931 (2011).
30. Silva, U. K., de, Brown, J. L. & Lapitsky, Y. Poly(allylamine)/tripolyphosphate coacervates enable high loading and multiple-month release of weakly amphiphilic anionic drugs: an in vitro study with ibuprofen. *RSC Adv.* **8**, 19409–19419 (2018).
31. Kolibaba, T. J. & Grunlan, J. C. Environmentally benign polyelectrolyte complex that renders wood flame retardant and mechanically strengthened. *Macromol. Mater. Eng.* **304**, 1900179 (2019).
32. Palen, B. et al. Clay-filled polyelectrolyte complex nanocoating for flame-retardant polyurethane foam. *ACS Omega* **6**, 8016–8020 (2021).
33. Horrocks, A. R. Chapter 1 - Fundamentals: Flammability, ignition, and fire spread in polymers. in *Analysis of Flame Retardancy in Polymer Science* (eds. Vahabi, H., Saeb, M. R. & Malucelli, G.) 1–72 (Elsevier), (2022).
34. Levchik, S. V. & Weil, E. D. A review on thermal decomposition and combustion of thermoplastic polyesters. *Polym. Adv. Technol.* **15**, 691–700 (2004).
35. Qi, L. et al. Durable flame retardant and dip-resistant coating of polyester fabrics by plasma surface treatment and UV-curing. *Prog. Org. Coat.* **172**, 107066 (2022).
36. Sonnier, R. Chapter 3 - Microscale forced combustion: Pyrolysis-combustion flow calorimetry (PCFC). in *Analysis of Flame Retardancy in Polymer Science* (eds. Vahabi, H., Saeb, M. R. & Malucelli, G.) 91–116 (Elsevier), (2022).
37. Lyon, R. E., Srafronava, N., Crowley, S. & Walters, R. N. A molecular-level fire growth parameter. *Polym. Degrad. Stab.* **186**, 109478 (2021).
38. Martín-Gullón, I., Esperanza, M. & Font, R. Kinetic model for the pyrolysis and combustion of poly-(ethylene terephthalate) (PET). *J. Anal. Appl. Pyrolysis* **58–59**, 635–650 (2001).
39. Zhang, J., Ji, Q., Zhang, P., Xia, Y. & Kong, Q. Thermal stability and flame-retardancy mechanism of poly(ethylene terephthalate)/boehmite nanocomposites. *Polym. Degrad. Stab.* **95**, 1211–1218 (2010).
40. Levchik, S. V. & Weil, E. D. Flame retardancy of thermoplastic polyesters—a review of the recent literature. *Polym. Int.* **54**, 11–35 (2005).

## ACKNOWLEDGEMENTS

The authors acknowledge the Texas A&M University Microscopy and Imaging Center Core Facility (RRID:SCR\_022128) for use of the SEM and the Texas A&M University Soft Matter Facility (RRID:SCR\_022482) for use of the Instron and TGA-MS.

## AUTHOR CONTRIBUTIONS

D.L.S.: conceptualization, investigation, writing – original draft, writing – review & editing, visualization. N.A.V.: investigation, visualization. M.O.C.: investigation, methodology. M.D.M.: investigation, visualization. J.C.G.: resources, guidance/mentorship, writing – review & editing.

## COMPETING INTERESTS

The authors declare no competing interests.

## ADDITIONAL INFORMATION

**Supplementary information** The online version contains supplementary material available at <https://doi.org/10.1038/s41529-024-00432-2>.

**Correspondence** and requests for materials should be addressed to Jaime C. Grunlan.

**Reprints and permission information** is available at <http://www.nature.com/reprints>

**Publisher's note** Springer Nature remains neutral with regard to jurisdictional claims in published maps and institutional affiliations.



**Open Access** This article is licensed under a Creative Commons Attribution 4.0 International License, which permits use, sharing, adaptation, distribution and reproduction in any medium or format, as long as you give appropriate credit to the original author(s) and the source, provide a link to the Creative Commons license, and indicate if changes were made. The images or other third party material in this article are included in the article's Creative Commons license, unless indicated otherwise in a credit line to the material. If material is not included in the article's Creative Commons license and your intended use is not permitted by statutory regulation or exceeds the permitted use, you will need to obtain permission directly from the copyright holder. To view a copy of this license, visit <http://creativecommons.org/licenses/by/4.0/>.

© The Author(s) 2024